9-8-2022

Partial Volumes of Phosphatidylcholines and Vitamin E: α-Tocopherol Prefers Disordered Membranes

Mitchell Dipasquale
University of Windsor

Michael H.L. Nguyen
University of Windsor

Georg Pabst
Universitat Graz

Drew Marquardt
University of Windsor

Partial volumes of Phosphatidylcholines and Vitamin E: α-Tocopherol Prefers Disordered Membranes

Mitchell DiPasquale,[†] Michael H. L. Nguyen,[†] Georg Pabst,[‡,¶] and Drew Marquardt[*,†,§]

†*Department of Chemistry and Biochemistry, University of Windsor, Windsor, Ontario, Canada*

‡*Institute of Molecular Biosciences, Biophysics Division, NAWI Graz, University of Graz, Graz, 8010, Austria*

¶*BioTechMed-Graz, Graz, 8010, Austria*

§*Department of Physics, University of Windsor, Windsor, Ontario, Canada*

E-mail: drew.marquardt@uwindsor.ca

Abstract

Despite its discovery over 95 years ago, the biological and nutritional roles of vitamin E remain subjects of much controversy. Though it is known to possess antioxidant properties, recent assertions have implied that vitamin E may not be limited to this function in living systems. Through densitometry measurements and small angle X-ray scattering we observe favorable interactions between α-tocopherol and unsaturated phospholipids, with more favorable interactions correlating to an increase in lipid chain unsaturation. Our data provide evidence that vitamin E may preferentially associate with oxygen sensitive lipids - an association that is considered innate for a viable membrane antioxidant.

Introduction

Cells have evolved to produce a staggering diversity of lipids, providing cellular membranes with a remarkable scope of functionality. Within the plasma membrane (PM) alone, hundreds of distinct lipid species organize to serve critical roles as both a barrier to the external environment, and as a solvent for the membrane's protein machinery.[1] A deeper understanding of membrane phenomena progresses the notion that cell membranes play a very active role in biology.

Evident from its foundational roles, membrane maintenance is crucial for cellular viability. Therefore, mechanisms must be present to mitigate the deterioration of lipid species that dictate membranes structure and, in consequence, membrane function. One of the most ubiquitous avenues of membrane damage is through reactive oxygen species (ROS), or oxidants. Aside from exogenous sources, endogenous ROS are regularly produced by various enzymatic and non-enzymatic pathways as required for cellular homeostasis. Notwithstanding, the introduction of ROS to cell membranes can adversely cause massive and rapid damage.[2–5]

Since its discovery in 1922, the biological significance of vitamin E (α-tocopherol) has been

mystified due to an array of conflicting reports.[6] Physiologically, vitamin E deficiency has been correlated to several health disorders including infertility,[7] and neuromuscular dysfunction,[8] yet clear molecular mechanisms for many of these responses remain elusive. Numerous studies have indicated α-tocopherol (αToc) as an antioxidant *in vitro*, often interpreting its function as a fat-soluble peroxyl radical scavenger,[9,10] yet, others have directly opposed this theory.[11] Studies have since diverged to show that αToc may in fact have critical roles in cellular processes such as signaling, apoptosis, protein activity, and gene regulation.[8,11–13] Considering the lack of conclusive evidence, the absence of a clear antioxidant health benefit from supplementation, and its significantly low physiological concentrations, skepticism continues to surround the true biological functions of vitamin E.[14]

As the most generally accepted role is that of an antioxidant, there are three physical aspects of vitamin E which are essential to justify an antioxidant mechanism: location, migration, and solubility. Vitamin E must properly orientate itself to perform as an antioxidant, be able to translate rapidly to the site of oxidation, and associate with oxidation-sensitive lipid environments. In fact, most recently the *in vitro* location of αToc has been used to reinforce its lipid-protecting role by demonstrating that its structure is oriented precisely in the membrane to intercept reactive free-radicals in addition to terminating chain oxidation reactions.[4,15,16]

Past studies have aimed to address the migration aspect of an antioxidant role. It has been suggested that sufficiently rapid lateral diffusion of αToc in the membrane could be a mechanism to compensate for low *in vitro* concentrations. To this end, Nau and co-workers used fluorescence quenching techniques to report that αToc does not significantly alter the lateral diffusion of phospholipids, and moreover, that αToc does not diffuse exceedingly fast compared to the phospholipids themselves.[17–19] These results have since largely been recapitulated *in silico*.[20]

Here, we begin to identify the interaction of vitamin E with different lipid environments by means of small angle X-ray scattering (SAXS) and densitometry, and thereby provide

the essential link between oxidation sensitive lipid membrane environments and the affinity of vitamin E. By incorporating αToc into a range of lipid vesicle systems of varying degrees of unsaturation and measuring the molecular volume of both the lipid and αToc using densitometry,[21] we observe the excess volume of mixing αToc, with SAXS measurements yielding barely distinguishable bilayer structures. Simply, a negative excess volume of mixing is indicative of a favourable interaction and a positive excess volume is an unfavourable interaction. Ultimately, the antioxidant hypothesis for vitamin E hinges upon a preferential association, and thereby a negative excess volume of mixing in oxygen-sensitive lipid environments.

Methods and Materials

Phospholipids were purchased from Avanti Polar Lipids (Alabaster, AL) and used as received. The lipids examined include 1,2-dipalmitoyl-sn-glycero-3-phosphocholine (DPPC, di-16:0PC), 1-palmitoyl-2-oleoyl-sn-glycero-3-phosphocholine (POPC, 16:0-18:1PC), 1,2-dioleoyl-sn-glycero-3-phosphocholine (DOPC, di-18:1PC), 1,2-dilinoleoyl-sn-glycero-3-phosphocholine (DLiPC, di-18:2PC). Sunflower phosphotydilcholine (SPC) extract was obtained from the American Lecithin Company (Oxford, CT). RRR-α-tocopherol was purchased from Sigma Aldrich (Milwaukee, WI) as an oil and was used as received.

Small Angle X-ray Scattering

For X-ray experiments, lipid stock solutions (DPPC, POPC, DOPC, and DLiPC) were prepared by dissolving predetermined amounts of dry lipids in chloroform. Phospholipid stock concentrations were verified by inorganic phosphate assay.[22]

Dry films were hydrated using 18 MΩcm^{-1} water by incubation for 2 h above the lipid melting temperature, with vortex mixing every 15 min. The final lipid concentration for each sample was $\approx$ 40 mg/mL.

Multilamellar vesicles (MLVs) were probed via small angle X-ray scattering (SAXS) to determine the bilayer structure. SAXS data were taken at the EMBL-BioSAXS P-12 beamline at DESY (Hamburg, Germany)[23] using 20 keV photons from the Petra U29 undulator and 2D photon counting Pilatus 2M pixel X-ray detector (Dectris). SAXS data were plotted, averaged, and background subtracted using ATSAS.[24]

Data were analyzed using the GAP framework and program put forward by Pabst et al..[25] In short, the transverse bilayer electron density profileis described by three Gaussian curves, producing a scattering amplitude that takes the form:

$$F(q) = 2\left[\sqrt{2\pi\sigma_h}\bar{\rho_H}e^{-\frac{\sigma_H^2 q^2}{2}}\cos(qz_H)\right] + \sqrt{2\pi\sigma_C}\bar{\rho_C}e^{-\frac{\sigma_C^2 q^2}{2}} \quad (1)$$

where $\bar{\rho_H}$ and $\bar{\rho_C}$ are the electron densities of the PC headgroup and the hydrocarbon tails relative to the electron density of a CH_2 group, respectively. The bilayer thickness ($d_B = 2(z_H + \sigma_H)$), water layer thickness ($d_w = d - d_B$), and the headgroup-headgroup distance ($d_{HH} = 2z_H$) were recoverable from the modeled data. We encourage the reader to review the work by Pabst et al.. for a more detailed derivation.[25,26]

Fityk was used to assist in indexing and refining the structural parameters of data exhibiting a modulated phase.[27]

Volume Measurements

Lipid dispersion for volume measurements were prepared by hydrating ≈ 25 mg of the desired lipid:αToc mixtures (0, 1, 2, 5, 10 and 20 mol% αToc) with ≈1.5 g of degassed ultrapure H_2O, obtained from a High-Q purification system (Wilmette, IL). Exact masses were carefully determined at each stage of the procedure. The lipid suspensions were then incubated at 50°C and gentle sonication was applied until the dispersion was uniformly "milky". SPC was used as a DLiPC surrogate for dilatometry measurements.* Neat α-tocopherol oil was also measured to complete the series.

*SPC is 85% 18:2 fatty acid chains.[28]

The temperature-dependent densities of water (ρ_w) and of the lipid dispersions (ρ_s), in the presence and absence of αToc, were determined by a temperature controlled Anton-Paar DMA5000 (Graz, Austria) vibrating tube densitometer. The temperature readout of the densitometer is within ± 0.001°C. Data from samples demonstrating bubble formation at high temperature measurements were discounted. The partial molecular volumes of lipid (V_L) and αToc ($V_{\alpha Toc}$)at a given temperature were calculated as previously established:[29]

$$\frac{N_A m_L}{MW_L} V_L + \frac{N_A m_{\alpha Toc}}{MW_{\alpha Toc}} V_{\alpha Toc} = \frac{m_L + m_{\alpha Toc} + m_W}{\rho_s} - \frac{m_W}{\rho_w} \tag{2}$$

where MW_L and $MW_{\alpha Toc}$ are the molecular weights of lipid and αToc, receptively, N_A is Avogadro's number, and m_L, $m_{\alpha Toc}$, and m_W are the masses of lipid, αToc, and water in the sample, respectively. In the absence of αToc, we see that the expression for a single lipid system is recovered. Given the mole fraction of αToc is:

$$\chi = \left(\frac{m_{\alpha Toc}}{MW_{\alpha Toc}} \right) \left(\frac{m_L}{MW_L} + \frac{m_{\alpha Toc}}{MW_{\alpha Toc}} \right)^{-1} \tag{3}$$

what is determined in the lipid–αToc binary systems is the average volume per molecule (V_χ).

$$V_\chi = \left(\frac{N_A m_L}{MW_L} + \frac{N_A m_{\alpha Toc}}{MW_{\alpha Toc}} \right)^{-1} \left(\frac{m_L + m_{\alpha Toc} + m_W}{\rho_s} - \frac{m_W}{\rho_w} \right) \tag{4}$$

Finally, the molecular volumes V_L and $V_{\alpha Toc}$ were determined by extrapolation of the linear fit to $V_\chi(\chi)$. We further quantified the effect of temperature on lipid and αToc volume by determining the thermal volume expansivities, $\alpha_V^T = \left(\frac{\partial V}{\partial T}\right)_\Pi V^{-1}$, where Π refers to constant surface pressure.[21]

Results

Bilayer Structure

SAXS data from fluid bilayers containing 10 mol% αToc indicate the existence of only a single lamellar phase. For this reason, a global small angle X-ray analysis of the MLVs suspensions was performed to assess membrane structural properties.[25,26] Data with GAP fits overlayed, equivalent to Fig. 1A, are provided in section S1 of the Supporting Information. Structural parameters determined for fluid L_α DPPC (50°C), POPC (20°C), DOPC (20°C), and DLiPC (20°C) in the presence and absence of 10 mol% αToc are summarized in Table 1 and expanded upon in Table S1. Modulated phases were observed in measurements from gel phase DPPC (20°C) in the presence of αToc. For this sample, Bragg scattering is indexed to identify coexisting phases and is in agreement with previous literature (SI Fig. S4).[30,31] The structural parameters for pure DPPC, POPC, and DOPC are in agreement with generally accepted structural parameters previously put forward; d_{HH} of DPPC, POPC, and DOPC have been reported as 38.4 Å, 37.4 Å, and 36.7 Å, respectively.[32–34]

For the unsaturated lipid samples, very minor changes are observed upon the addition of αToc, which are quantified by changes in structural parameters (Table 1) and can be visualized as deviations in the transbilayer electron density profiles provided in Fig. 1. For example, addition of αToc drives a slight increase in membrane lamellar periodicity d, except for DOPC. The increase in d does not greatly influence the bilayer thickness d_B, but is instead largely accounted for by an increase in the interlamellar water layer thickness d_W. A large d_W for DPPC in comparison to the other samples was expected due to the elevated temperature required for L_α measurements. The exception to these observations is DOPC, which experiences bilayer thickening with decreased interbilayer hydration.

Of particular interest is the observable increase in the Caillé fluctuation parameter η upon addition of αToc to all fluid bilayers, although the changes for DOPC are within error (Table S1). In the Modified Calillé Theory (MCT) model, the fluctuation parameter accounts for

the decay of positional correlations as a result of membrane bending fluctuations.[35,36] This measurement of microviscosity is a convolution of both the membrane elastic bending and compression moduli and can thus vaguely comment on membrane rigidity. An increase in η across all lipids suggests that L_α phase bilayers become more fluid, or softer, in the presence of αToc, or a decrease of the compression modulus due to a softening of the bilayer interaction potential.

Table 1: Structural parameters determined from GAP analysis of SAXS data for L_α phospholipid bilayers in the presence and absence of 10 mol% αToc. Typical error for d is $\pm$ 0.01 Å for all measurements, and is $\lesssim$ 1.5% for d_{HH} and $\lesssim$ 2.5% for d_W. For more detail on structural parameters derived from GAP analysis, including specific error, consult Table 1. of the SI.

	d (Å)	z_H (Å)	σ_C (Å)	d_{HH} (Å)	d_W (Å)	η ($\times 10^{-2}$)
DPPC	65.2	18.8	5.6	37.6	21.7	8.2
+ αToc	66.2	18.5	6.2	36.9	23.3	9.5
POPC	63.7	18.4	6.7	36.8	14.9	6.4
+ αToc	65.0	18.8	6.7	37.6	15.5	7.3
DOPC	62.3	18.1	5.9	36.1	14.2	5.3
+ αToc	62.3	18.7	5.3	37.4	12.9	5.5
DLiPC	61.4	17.1	6.2	34.2	15.2	8.7
+ αToc	62.8	17.1	7.0	34.3	16.6	9.8

Lipid Volumes and Thermal Expansion

Our determined volumes of pure lipid systems are in agreement with previously reported values and are summarized and compared in Table S2 of the SI.[33,37] In fact, values extracted from densitometry readings are within $< 1\%$ of the values determined via the centrifugation method outlined in Greenwood et al., thereby reinforcing the validity of this technique.[37]

As depicted as linear regressions to Fig. 2A, molecular volumes of each lipid species in the presence of αToc are extrapolated and tabulated in Table 2. When compared to neat lipid bilayers, data show no significant alteration in lipid volume upon the incorporation of

αToc, including DPPC at temperatures below the main phase transition. In fact, the lipid volume in the presence of αToc deviates less than 0.5% from the measured volume of pure lipid. Figure 2B illustrates the temperature-dependent linear increase in the lipid molecular volume V_L in the presence of αToc. Also highlighted in this figure is the prevalent volume expansion that occurs when DPPC undergoes its main $L_\beta \rightarrow L_\alpha$ phase transition, which is observed in the region one would expect the pure lipid ($\approx 42°C$)[38,39] and has previously been demonstrated using dilatometry.[40]

Table 2: Temperature dependence of lipid and αToc partial volumes (A^3) for different PC bilayers containing αToc. A volume uncertainty of 0.3% was estimated based on replicate densitometry measurements before and after sample dilution.

	DPPC		POPC		DOPC		SPC	
	V_L	$V_{\alpha Toc}$	V_L	$V_{\alpha Toc}$	V_L	$V_{\alpha Toc}$	V_L	$V_{\alpha Toc}$
20 °C	**1132.1**	**985.6**	1238.6	741.2	1291.7	722.7	1245.0	724.7
30 °C	**1144.9**	**911.7**	1248.9	743.5	1300.7	733.3	1251.2	727.7
40 °C	-	-	1258.7	748.2	1311.1	738.5	1256.0	727.5
50 °C	1219.1	763.1	1268.8	752.1	-	-	1259.5	727.7

Bolded values indicate measurements taken in the L_β phase.

Isobaric thermal expansivities of phospholipids $\alpha^T_{V_L}$ and expansion rates $\frac{\partial V}{\partial T}$ in the presence and absence of αToc are derived from the slope of linear fits to Fig. 2B and collected in Table 3. For fluid phase bilayers, the introduction of αToc imposes a dramatic suppression of the expansion of increasingly disordered bilayer environments. No difference is observed in the expansion behaviour of POPC, but the volume expansion rate of DOPC (two degrees of unsaturation per lipid) is decreased by $\approx 20\%$ and SPC (DLiPC surrogate; > 3 double bonds per lipid) is nearly halved in the presence of αToc. The thermal expansion rate of αToc oil was measured directly to be 0.55 ± 0.01 Å^3 K^{-1}.

Partial Volume of α-Tocopherol

By extrapolating the data of Fig. 2A toward the unity of αToc, the partial molecular volume of αToc is extracted. Unlike the phospholipids examined, the partial molecular volume of

Table 3: Fluid phase isobaric volume thermal expansivity $\alpha^T_{V_L}$ ($\times 10^{-4}$ $\mathbf{K}^{-1}$) at 40°C and expansion rate $\frac{\partial V}{\partial T}$ ($\mathbf{Å}^3$ $\mathbf{K}^{-1}$) different PC bilayers in the presence and absence of αToc.

	Neat		+ αToc		Literature	
	$\frac{\partial V}{\partial T}$	$\alpha^T_{V_L}$	$\frac{\partial V}{\partial T}$	$\alpha^T_{V_L}$	$\frac{\partial V}{\partial T}$	$\alpha^T_{V_L}$
DPPC	1.10 ± 0.03	9.03 ± 0.24[a]	1.10 ± 0.08	9.02 ± 0.66[a]	(1.30)[b]	10.50[b]
POPC	0.98 ± 0.01	7.74 ± 0.32	1.00 ± 0.01	7.98 ± 0.29	1.00 ± 0.04[c]	8.02 ± 0.34[c]
DOPC	1.21 ± 0.06	9.23 ± 0.73	0.97 ± 0.04	7.40 ± 0.53	1.22 ± 0.03[d]	9.40 ± 0.21[d]
SPC	0.96 ± 0.01	7.61 ± 0.27	0.49 ± 0.03	3.86 ± 0.38	-	-

[a] Calculated at 50°C.

[b] Derived from reference Raudino et al. at 70°C and 100mM NaCl.[41] Note that the rate is estimated based on our thermal expansion parameter.

[c] Derived from Koenig and Gawrisch.[42]

[d] Derived from Uhríková et al..[43]

αToc is influenced by the lipid environment in which it resides. The volumes of αToc in different lipid environments are provided in Table 2 and plotted in Fig. 2C. At physiological temperatures (30°C–40°C) the data would suggest that the molecular volume decreases with increasing unsaturation of the host phospholipid. In other words, the volume contracts in progressively disordered bilayers. As illustrated in Fig. 3, the contraction phenomenon is most apparent for DPPC below its chain melting transition. In this instance, the volume of αToc is $\approx$ 20% larger in the gel phase relative to its volume in a fluid lipid at the same temperature. For small mole fractions of αToc, such as ours, the extrapolated V_L does not account for the condensation effect that αToc has on the system. As outlined in Greenwood et al. for cholesterol, our $V_{\alpha Toc}$ accounts for the both the neat volume of αToc as well as the condensation (or expansion) of the lipid.[37] In other words, the condensation at low concentrations of αToc is observed in $V_{\alpha Toc}$ and not V_L.

Discussion

Tocopherol Modifies Bilayer Properties

Many membrane components that serve a structural role exert an observable change on the structure of the bilayer. Particularly, in fluid lipid bilayers with bulk concentrations

that are substantially ($\approx$ 10-100$\times$)[44] higher than *in vivo* we observe no significant structural perturbation caused by the presence of α-tocopherol (Fig. 1). These SAXS results reported in Table 1 are in good agreement with previous work on similar compositions and we reaffirm that αToc does not influence bilayer structure at the studied concentrations.[30,45] Interestingly, while bilayers appear architecturally similar, the addition of αToc introduces a more pertinent change in both the interbilayer water thickness d_W and the Caillé fluctuation parameter η.

For all fluid phase bilayers studied, an increase in η with minimal perturbation on bilayer structure leads to speculation that the addition of αToc influences the behaviour of the acyl chains. Introduction of tocopherol to lipid membranes has been shown by ^{2}H NMR to reduce the degrees of freedom in the host acyl chains, as measured as an increase in chain segment order parameter profiles.[15,46]

Membrane rigidity is inversely correlated to the area per lipid, such that lower lateral lipid density signifies softer membranes.[47–49] An increase in chain thickness, as is the case with cholesterol inclusion, produces an increase in membrane rigidity.[49] This should correspond to an increase in area per lipid; however, the reduction in molecular volume presumes a condensation effect that theoretically increases rigidity.

Clearly, this is not correlated to our measured values of η, which increased for all studied lipids independent of increased or decreased lipid packing densities. This suggests that either the polymer brush model does not apply to all lipid αToc mixtures, or that *eta* increases due to a softening of the bilayer interaction potential (e.g. due to decreased van der Waals attraction). Note, Doktorova et al. recently demonstrated that the linearity of the polymer brush model of cholesterol/lipid mixtures can be restored by redefining the mechanical thickness of the lipid bilayer. A similar scenario might apply to αToc/lipid mixtures.

Taken together, these observations are in line with the proposed location and orientation of αToc in bilayers with the reducing hydroxyl moiety directed toward the interface and

the phytyl tail penetrating into the hydrophobic core.[4,45,46] For DPPC, POPC, and a PUFA lipid, tocopherol sits at the same depth and thus imparts a similar physical distortion on the host membrane.

The exception to these trends is DOPC, which responds to the addition of αToc with an increase in d_{HH} and a decrease in d_W coupled to a relatively idle change in η. This describes a slightly thicker membrane with a maintained rigidity, but reduces the hydrating layer. These trends again align with the observation by Marquardt et al. that tocopherol sits slightly deeper in DOPC membranes, providing an explanation where αToc has a greater influence on intrabilayer properties and less effect on the interfacial region.[4] Interestingly, this structural influence by αToc has many parallels to the condensing effect of cholesterol on DOPC as recently explored by Chakraborty et al..[49] In spite of the similar increase in bilayer steric thickness, η suggests that αToc does not increase membrane rigidity like was found for cholesterol.

From SAXS studies on gel DPPC, αToc appears to have a influence on bilayer structure at temperatures below the lipid main melting transition. Previous X-ray diffraction studies on supported multibilayer stacks has shown co-existence between the gel phase ($L_{\beta'}$) and the symmetric ripple phase (P_β) in DPPC bilayers containing 10 mol% αToc at 20°C.[30] In our free floating MLVs (DPPC+10 mol% αToc) we observe three-phase co-existence in DPPC bilayers at 20°C. Similar to data from supported multibilayer stacks, we observe the $L_{\beta'}$ and P_β, but in addition we observe the emergence of the asymmetric ripple phase ($P_{\beta'}$). The presence of the $P_{\beta'}$ could be a result of free-floating MLVs as opposed to supported stacks, the level of hydration, or a heterogeneous distribution of αToc among MLVs in the sample preparation. Nevertheless, it is clear that αToc induces modulated phases of phospholipid bilayers in non-fluid bilayers.

Other reports of αToc in DPPC at low temperatures do not specifically demonstrate the presence of modulated phases. For example, Ausili et al. investigate DPPC MLV systems at 20 mol% tocopherol, and suggest a superimposition of wide angle scattering peaks from

coexisting L_β and L_α phases, without conclusively reporting the induction of modulated phases.[45] This discrepancy could simply arise from resolution limitations of the home-source instrumentation used to probe their system, as compared to the synchrotron radiation data presented here. Notably, the optics configuration employs Kratky camera for a line-shaped beam which can lead to significant smearing effects at low q, thereby obscuring observation of modulated phases.

In di-saturated lipid bilayers, tocopherol-induced phase modulation has been proposed to lead to lipid curvature coupling which drives enrichment of tocopherol in the vertices of the ripple phase.[51] It is worth noting that this clustering is not observed in our present studies on L_α bilayers, nor the work of others,[30,45,52] and thus it calls into questions the significance of this behaviour in relation to an antioxidant mechanism. This behaviour does however suggest an unfavourable mixing interaction of αToc with highly ordered gel-phase di-saturated lipids.

Tocopherol Prefers Disordered Environments

In previous studies, the affinity of cholesterol for ordered environments was argued, in part, from studies probing the mixing behaviour of cholesterol in progressively saturated lipid membranes. Greenwood et al. described the contraction in molecular volume of cholesterol relative to an idealized V_{chol} when incorporated into bilayers composed of the di-saturated lipids DPPC and di-14:0PC.[37] Contrarily, when mixed with more disordered lipids such as DOPC and POPC, V_{chol} demonstrated a slight expansion beyond the idealized molecular volume which indicates an unfavourable interaction. These observations have since been supplemented by simulation and validated through additional thermodynamic and biophysical studies.[53–55]

In this work, we describe a volumetric trend of α-tocopherol that directly contrasts the behaviour of cholesterol. In highly ordered di-saturated lipid environments (gel phase DPPC) αToc exhibits a dramatic expansion in $V_{\alpha Toc}$. The high variability of $V_{\alpha Toc}$ with temperature

in the L_β phase (Fig. 2C; open squares) could arise from the aforementioned clustering of tocopherol into modulated phases as observed by SAXS. Any measurement of $V_{\alpha Toc}$ in L_α phase bilayers displayed a contraction in molecular volume, which was amplified in progressively unsaturated bilayers. This trend with unsaturation was reflected in measurements of thermal expansivity $\alpha^T_{V_L}$ which is dramatically suppressed when αToc is introduced to disordered environments (Table 3). In fact, $\alpha^T_{V_L}$ is more than halved when doped into SPC; a highly unsaturated natural phosphatidylcholine extract.[28] This suggests that αToc has a stabilizing influence on disordered membranes.

At 25 °C an idealized molecular volume of αToc is calculated to be $V_{\alpha Toc} = 753$ Å^3. We report a contraction in molecular volume in progressively disordered lipid environments which appears to approach ≈ 725 Å^3 as a measure of the bare volume of αToc in lipid bilayers (Fig. 3). These observations complement the work of others to advocate that αToc preferentially associates with PUFA-containing lipids —an association that is inherent to its putative function as an antioxidant.[45,52,56,57]

Contrasting our work, recent molecular dynamics simulations propose that αToc has a greater affinity for a less saturated lipid (18:0-18:1PC, SOPC) as compared to a PUFA lipid (18:0-22:6PC,SDPC).[58] While this is largely based on an enthalpic benefit of binding αToc to SOPC, the complementary parameters derived from their simulations describe a strong entropic benefit to αToc association with SDPC-rich environments. These substantial increases in dynamic processes such as diffusion and flip-flop not only indicate that αToc has no aversion for the disordered environment, but are also highly conducive to an antioxidant mechanism wherein αToc is able to transiently associate with, and thereby protect, a greater lipid population.

As a caveat, Wang and Quinn report that tocopherol preferentially partitions into PC rich lipid domains rather than phosphoethanolamine, irrespective of the unsaturation.[59] This headgroup dependence cannot go unnoticed when discussing vitamin E as a biological antioxidant since it has been shown that PUFA chains are more likely to be attached to a

phosphoethanolamine headgroup in red blood cells.[60–64] Here, we did not investigate different lipid headgroups; rather, by maintaining a constant headgroup our data clearly illustrate a reduction in αToc volume, indicating a favorable interaction that directly correlates to chain unsaturation.

At the chemical level, cholesterol can serve as a radical scavenger and has been associated with an antioxidant function in early air-breathing creatures.[55,65,66] From an evolutionary standpoint, perhaps vitamin E overtook cholesterol as the choice lipophilic antioxidant of biology due to the preferential partitioning of the two molecules, wherein vitamin E sequesters to the disordered unsaturated membrane environments provided by oxygen sensitive lipids. This relationship between tocopherol and cholesterol is only beginning to be explored, and perhaps the partitioning is further exasperated when dopants compete for phases.[67,68] As a launching point, our data demonstrate that αToc has increasingly favorable interactions with lipids containing greater degrees of unsaturation.

Conclusion

The presence of αToc has a minimal impact on the structure and molecular volume of the fluid phospholipid bilayer in which it resides. This lends credence to the argument that vitamin E does not serve a structural role *in vivo*. Most significantly, an affinity between αToc and disordered lipids was established through molecular volume measurements yielding a negative excess volume of mixing for αToc in progressively unsaturated lipid systems. Together, this work supports the plausibility of α-tocopherol as an antioxidant by providing experimental evidence of an affinity of αToc toward oxidation-sensitive lipid environments.

Acknowledgement

The authors thank Clement Blanchet for SAXS technical assistance and Thad Harroun for discussions. The research leading to these results has received funding from the European

Community's Seventh Framework Programme (FP7/2007-2013) under BioStruct-X (grant agreement No. 6042.12). MD and MHLN are recipients Canada Graduate Scholarship - Doctoral Awards (CGS-D) through CIHR and NSERC, respectively. DM acknowledges the support of the Natural Sciences and Engineering Research Council of Canada (NSERC), [funding reference number 2018-04841] and the University of Windsor startup funds.

Supporting Information Available

Analyzed SAXS structural data and tabulated pure lipid volumes can be found in Supporting Information.

This material is available free of charge via the Internet at `http://pubs.acs.org/`.

References

(1) Singer, S. J.; Nicolson, G. L. The Fluid Mosaic Model of the Structure of Cell Membranes. *Science* **1972**, *175*, 720–731.

(2) Yusupov, M.; Wende, K.; Kupsch, S.; Neyts, E. C.; Reuter, S.; Bogaerts, A. Effect of head group and lipid tail oxidation in the cell membrane revealed through integrated simulations and experiments. *Sci. Rep.* **2017**, 5761.

(3) Tsubone, T. M.; Junqueira, H. C.; Baptista, M. S.; Itri, R. Contrasting roles of oxidized lipids in modulating membrane microdomains. *Biochim. Biophys. Acta - Biomembr.* **2019**, *1861*, 660–669.

(4) Marquardt, D.; Williams, J. A.; Kučerka, N.; Atkinson, J.; Wassall, S. R.; Katsaras, J.; Harroun, T. A. Tocopherol Activity Correlates with Its Location in a Membrane: A New Perspective on the Antioxidant Vitamin E. *J. Am. Chem. Soc.* **2013**, *135*, 7523–7533.

(5) Marquardt, D.; Heberle, F. A.; Pan, J.; Cheng, X.; Pabst, G.; Harroun, T. A.; Kučerka, N.; Katsaras, J. The structures of polyunsaturated lipid bilayers by joint refinement of neutron and X-ray scattering data. *Chem. Phys. Lipids* **2020**, *229*, 104892.

(6) Atkinson, J.; Marquardt, D.; DiPasquale, M.; Harroun, T. From fat to bilayers: Understanding where and how vitamin E works. *Free Radic. Biol. Med.* **2021**, *176*, 73–79.

(7) Evans, H. M.; Bishop, K. S. On The Existence Of A Hitherto Unrecognized Dietary Factor Essential For Reproduction. *Science* **1922**, *56*, 650–651.

(8) Gohil, K.; Vash, V. T.; Cross, C. E. Dietary α-tocopherol and neuromuscular health: Search for optimal dose and molecular mechanisms continues! *Mol. Nutr. Food. Res.* **2010**, *54*, 693–709.

(9) Buettner, G. R. The Pecking Order of Free Radicals and Antioxidants: Lipid Peroxidation, alpha-Tocopherol and Ascorbate. *Arch. Biochem. Biophys.* **1993**, *300*, 535–543.

(10) Niki, E. Lipid oxidation that is, and is not, inhibited by vitamin E: Consideration about physiological functions of vitamin E. *Free Radic. Biol. Med.* **2021**, *176*, 1–15.

(11) Azzi, A. Molecular mechanism of alpha-tocopherol action. *Free Radicals Biol. Med.* **2007**, *43*, 16–21.

(12) Noguchi, N.; Hanyu, R.; Nonaka, A.; Okimoto, Y.; Kodama, T. Inhibition of THP-1 cell adhesion to endothelial cells by α-tocopherol and α-tocotrienol is dependent on intracellular concentration of the antioxidants. *Free Radic. Biol. Med.* **2003**, *34*, 1614 – 1620.

(13) Azzi, A. Reflections on a century of vitamin E research: Looking at the past with an eye on the future. *Free Radic. Biol. Med.* **2021**, *175*, 155–160.

(14) Brigelius-Flohé, R. Vitamin E research: Past, now and future. *Free Radic. Biol. Med.* **2021**, *177*, 381–390.

(15) Leng, X.; Kinnun, J. J.; Marquardt, D.; Ghefli, M.; Kučerka, N.; Katsaras, J.; Atkinson, J.; Harroun, T. A.; Feller, S. E.; Wassall, S. R. α-Tocopherol Is Well Designed to Protect Polyunsaturated Phospholipids: MD Simulations. *Biophys. J.* **2015**, *109*, 1608–1618.

(16) Marquardt, D.; Kučerka, N.; Katsaras, J.; Harroun, T. A. α-Tocopherol's Location in Membranes Is Not Affected by Their Composition. *Langmuir* **2015**, *31*, 4464–4472.

(17) Gramlich, G.; Zhang, J.; Nau, W. M. Diffusion of α-Tocopherol in Membrane Models: Probing the Kinetics of Vitamin E Antioxidant Action by Fluorescence in Real Time. *J. Am. Chem. Soc.* **2004**, *126*, 5482–5492.

(18) Sonnen, A. F.-P.; Bakirci, H.; Netscher, T.; Nau, W. M. Effect of Temperature, Cholesterol Content, and Antioxidant Structure on the Mobility of Vitamin E Constituents in Biomembrane Models Studied by Laterally Diffusion-Controlled Fluorescence Quenching. *J. Am. Chem. Soc.* **2005**, *127*, 15575–15584.

(19) Meyer, R.; Sonnen, A. F.-P.; Nau, W. M. Phase-Dependent Lateral Diffusion of α-Tocopherol in DPPC Liposomes Monitored by Fluorescence Quenching. *Langmuir* **2010**, *26*, 14723–14729.

(20) Qin, S.-S.; Yu, Z.-W.; Yu, Y.-X. Structural and Kinetic Properties of α-Tocopherol in Phospholipid Bilayers, a Molecular Dynamics Simulation Study. *J. Phys. Chem. B.* **2009**, *113*, 16537–16546.

(21) Pan, J.; Heberle, F. A.; Tristram-Nagle, S.; Szymanski, M.; Koepfinger, M.; Katsaras, J.; Kučerka, N. Molecular structures of fluid phase phosphatidylglycerol bilayers as determined by small angle neutron and X-ray scattering. *Biochim. Biophys. Acta* **2012**, *1818*, 2135–2148.

(22) Kingsley, P.; Feigenson, G. The synthesis of a perdeuterated phospholipid: 1,2-dimyristoyl-*sn*-glycero-3-phosphocholine-$d_7$2. *Chem. Phys. Lipids* **1979**, *24*, 135–147.

(23) Blanchet, C. E.; Spilotros, A.; Schwemmer, F.; Graewert, M. A.; Kikhney, A.; Jeffries, C. M.; Franke, D.; Mark, D.; Zengerle, R.; Cipriani, F. et al. Versatile sample environments and automation for biological solution X-ray scattering experiments at the P12 beamline (PETRA III, DESY). *J. Appl. Crystallogr.* **2015**, *48*, 431–443.

(24) Petoukhov, M. V.; Franke, D.; Shkumatov, A. V.; Tria, G.; Kikhney, A. G.; Gajda, M.; Gorba, C.; Mertens, H. D. T.; Konarev, P. V.; Svergun, D. I. New developments in the ATSAS program package for small-angle scattering data analysis. *J. Appl. Crystallogr.* **2012**, *45*, 342–350.

(25) Pabst, G.; Rappolt, M.; Amenitsch, H.; Laggner, P. Structural information from multilamellar liposomes at full hydration: Full q-range fitting with high quality x-ray data. *Phys. Rev. E* **2000**, *62*, 4000–4009.

(26) Pabst, G.; Katsaras, J.; Raghunathan, V. A.; Rappolt, M. Structure and Interactions in the Anomalous Swelling Regime of Phospholipid Bilayers. *Langmuir* **2003**, *19*, 1716–1722.

(27) Wojdyr, M. *Fityk*: a general-purpose peak fitting program. *J. Appl. Crystallogr.* **2010**, *43*, 1126–1128.

(28) Orsavova, J.; Misurcova, L.; Ambrozova, J. V.; Vicha, R.; Mlcek, J. Fatty Acids Composition of Vegetable Oils and Its Contribution to Dietary Energy Intake and Dependence of Cardiovascular Mortality on Dietary Intake of Fatty Acids. *Int. J. Mol. Sci.* **2015**, *16*, 12871–12890.

(29) Pan, J.; Cheng, X.; Heberle, F. A.; Mostofian, B.; Kučerka, N.; Drazba, P.; Katsaras, J. Interactions between Ether Phospholipids and Cholesterol As Determined by Scattering and Molecular Dynamics Simulations. *J. Phys. Chem. B.* **2012**, *116*, 14829–14838.

(30) Kamal, M. A.; Raghunathan, V. Modulated phases of phospholipid bilayers induced by tocopherols. *Biochim. Biophys. Acta - Biomembr.* **2012**, *1818*, 2486 – 2493.

(31) Rappolt, M.; Rapp, G. Structure of the stable and metastable ripple phase of dipalmitoylphosphatidylcholine. *Eur. Biophys. J.* **1996**, *24*, 381–386.

(32) Kučerka, N.; Nagle, J. F.; Sachs, J. N.; Feller, S. E.; Pencer, J.; Jackson, A.; Katsaras, J. Lipid bilayer structure determined by the simultaneous analysis of neutron and X-ray scattering data. *Biophys. J.* **2008**, *95*, 23562367.

(33) Kučerka, N.; Nieh, M.-P.; Katsaras, J. Fluid phase lipid areas and bilayer thicknesses of

commonly used phosphatidylcholines as a function of temperature. *Biochim. Biophys. Acta* **2011**, *1808*, 2761–2771.

(34) Heftberger, P.; Kollmitzer, B.; Heberle, F. A.; Pan, J.; Rappolt, M.; Amenitsch, H.; Kučerka, N.; Katsaras, J.; Pabst, G. Global small-angle X-ray scattering data analysis for multilamellar vesicles: the evolution of the scattering density profile model. *J. Appl. Crystallogr.* **2014**, *47*, 173–180.

(35) Pabst, G.; Koschuch, R.; Pozo-Navas, B.; Rappolt, M.; Lohner, K.; Laggner, P. Structural analysis of weakly ordered membrane stacks. *J. Appl. Crystallogr.* **2003**, *36*, 1378–1388.

(36) Pabst, G. Global Properties of Biomimetic Membranes: Perspecives on Molecular Features. *Biophys. Rev. Lett.* **2006**, *01*, 57–84.

(37) Greenwood, A. I.; Tristram-Nagle, S.; Nagle, J. F. Partial molecular volumes of lipids and cholesterol. *Chem. Phys. Lipids* **2006**, *143*, 1–10.

(38) Mabrey, S.; Sturtevant, J. M. Investigation of phase transitions of lipids and lipid mixtures by high sensitivity differential scanning calorimetry. *Proc. Natl. Acad. Sci. U. S. A.* **1976**, *73*, 3862–3866.

(39) Marquardt, D.; Heberle, F. A.; Miti, T.; Eicher, B.; London, E.; Katsaras, J.; Pabst, G. 1H NMR Shows Slow Phospholipid Flip-Flop in Gel and Fluid Bilayers. *Langmuir* **2017**, *33*, 3731–3741.

(40) Kharakoz, D. P.; Shlyapnikova, E. A. Thermodynamics and Kinetics of the Early Steps of Solid-State Nucleation in the Fluid Lipid Bilayer. *J. Phys. Chem. B.* **2000**, *104*, 10368–10378.

(41) Raudino, A.; Zuccarello, F.; La Rosa, C.; Buemi, G. THermal Expansion and Com-

pressibility Coefficients of Phospholipid Vesicles. Experimental Determination adn Theoretical Modeling. *J. Phys. Chem.* **1990**, *94*, 4217–4223.

(42) Koenig, B. W.; Gawrisch, K. Specific volumes of unsaturated phosphatidylcholines in the liquid crystalline lamellar phase. *Biochim. Biophys. Acta - Biomembr.* **2005**, *1715*, 65–70.

(43) Uhríková, D.; Rybár, P.; Hianik, T.; Balgavý, P. Component volumes of unsaturated phosphatidylcholines in fluid bilayers: a densitometric study. *Chem. Phys. Lipids* **2007**, *145*, 97–105.

(44) Atkinson, J.; Epand, R. F.; Epand, R. M. Tocopherols and tocotrienols in membranes: A critical review. *Free Radic. Biol. Med.* **2008**, *44*, 739–764.

(45) Ausili, A.; Torrecillas, A.; de Godos, A. M.; Corbaln-Garca, S.; Gmez-Fernndez, J. C. Phenolic Group of α-Tocopherol Anchors at the LipidWater Interface of Fully Saturated Membranes. *Langmuir* **2018**, *34*, 3336–3348.

(46) Marquardt, D.; Williams, J. A.; Kinnun, J. J.; Kučerka, N.; Atkinson, J.; Wassall, S. R.; Katsaras, J.; Harroun, T. A. Dimyristoyl phosphatidylcholine: a remarkable exception to α-tocopherol's membrane presence. *J. Am. Chem. Soc.* **2014**, *136*, 203–210.

(47) Evans, E.; Rawicz, W. Entropy-driven tension and bending elasticity in condensed-fluid membranes. *Phys. Rev. Lett.* **1990**, *64*, 2094–2097.

(48) Kelley, E. G.; Butler, P. D.; Ashkar, R.; Bradbury, R.; Nagao, M. Scaling relationships for the elastic moduli and viscosity of mixed lipid membranes. *Proc. Natl. Acad. Sci. U.S.A.* **2020**, *117*, 23365–23373.

(49) Chakraborty, S.; Doktorova, M.; Molugu, T. R.; Heberle, F. A.; Scott, H. L.; Dzikovski, B.; Nagao, M.; Stingaciu, L.-R.; Standaert, R. F.; Barrera, F. N. et al.

How cholesterol stiffens unsaturated lipid membranes. *Proc. Natl. Acad. Sci. U.S.A.* **2020**, *117*, 21896–21905.

(50) Doktorova, M.; LeVine, M. V.; Khelashvili, G.; Weinstein, H. A New Computational Method for Membrane Compressibility: Bilayer Mechanical Thickness Revisited. *Biophys. J.* **2019**, *116*, 487–502.

(51) Quinn, P. J. Is the Distribution of α-Tocopherol in Membranes Consistent with Its Putative Functions? *Biochemistry (Moscow)* **2004**, *69*, 58–66.

(52) Ausili, A.; de Godos, A. M.; Torrecillas, A.; Aranda, F. J.; Corbalan-Garcia, S.; Gomez-Fernandez, J. C. The vertical location of α-tocopherol in phosphatidylcholine membranes is not altered as a function of the degree of unsaturation of the fatty acyl chains. *Phys. Chem. Chem. Phys.* **2017**, *19*, 6731–6742.

(53) Niu, S.-L.; Litman, B. J. Determination of Membrane Cholesterol Partition Coefficient Using a Lipid Vesicle-Cyclodextrin Binary System: Effect of Phospholipid Acyl Chain Unsaturation and Headgroup Composition. *Biophys. J.* **2002**, *83*, 3408–3415.

(54) Tsamaloukas, A.; Szadkowska, H.; Heerklotz, H. Thermodynamic comparison of the interactions of cholesterol with unsaturated phospholipid and sphingomyelins. *Biophys. J.* **2006**, *90*, 4479–4487.

(55) Marquardt, D.; Kučerka, N.; Wassall, S. R.; Harroun, T. A.; Katsaras, J. Cholesterol's location in lipid bilayers. *Chem. Phys. Lipids* **2016**, *199*, 17 – 25.

(56) Atkinson, J.; Harroun, T.; Wassall, S. R.; Stillwell, W.; Katsaras, J. The location and behavior of αtocopherol in membranes. *Molecular Nutrition & Food Research* **2010**, *54*, 641–651.

(57) Williams, J. A.; LoCascio, D. S.; Tsamaloukas, A.; Heerklotz, H.; Stillwell, W.; Was-

sall, S. R. Preferential Interaction of α-tocopherol with PUFA-containing Lipids Characterized by Isothermal Titration Calorimetry. *Biophys. J.* **2009**, *96*, 608a.

(58) Leng, X.; Zhu, F.; Wassall, S. R. Vitamin E Has Reduced Affinity for a Polyunsaturated Phospholipid: An Umbrella Sampling Molecular Dynamics Simulations Study. *J. Phys. Chem. B.* **2018**, *122*, 8351–8358.

(59) Wang, X.; Quinn, P. J. Preferential interaction of α-tocopherol with phosphatidylcholines in mixed aqueous dispersions of phosphatidylcholine and phosphatidylethanolamine. *Eur. J. Biochem.* **2000**, *267*, 6362–6368.

(60) Essaid, D.; Rosilio, V.; Daghildjian, K.; Solgadi, A.; Vergnaud, J.; Kasselouri, A.; Chaminade, P. Artificial plasma membrane models based on lipidomic profiling. *Biochim. Biophys. Acta - Biomembr.* **2016**, *1858*, 2725 – 2736.

(61) Ma, D.; Arendt, B.; Hillyer, L.; Fung, S.; McGilvray, I.; Guindi, M.; Allard, J. Plasma phospholipids and fatty acid composition differ between liver biopsy-proven nonalcoholic fatty liver disease and healthy subjects. *Nutrition and Diabetes* **2016**, *e220*, 1 – 7.

(62) Dodge, J. T.; Phillips, G. B. Composition of phospholipids and of phospholipid fatty acids and aldehydes in human red cells. *Journal of Lipid Research* **1967**, *8*, 667 – 675.

(63) Klem, S.; Klingler, M.; Demmelmair, H.; Koletzko, B. Efficient and Specific Analysis of Red Blood Cell Glycerophospholipid Fatty Acid Composition. *PLOS ONE* **2012**, *7*, 1–8.

(64) Akinyemi, O.; Bruckner, G.; Johnson, J.; Lennie, T. A.; Hildebrand, D. A Rapid and Simple Method for Fatty Acid Profiling and Determination of ω-3 Index in Red Blood Cells. *Open Nutr J* **2017**, *11*, 17 – 26.

(65) Smith, L. L. Another cholesterol hypothesis: Cholesterol as antioxidant. *Free Radicals Biol. Med.* **1991**, *11*, 47–61.

(66) Brown, A. J.; Galea, A. M. Cholesterol as an evolutionary response to living with oxygen. *Evolution (Hoboken, NJ, U. S.)* **2010**, *64*, 2179–2183.

(67) DiPasquale, M.; Nguyen, M. H.; Rickeard, B. W.; Cesca, N.; Tannous, C.; Castillo, S. R.; Katsaras, J.; Kelley, E. G.; Heberle, F. A.; Marquardt, D. The antioxidant vitamin E as a membrane raft modulator: Tocopherols do not abolish lipid domains. *Biochim. Biophys. Acta - Biomembr.* **2020**, *1862*, 183189.

(68) Wassall, S. R.; Stillwell, W. Docosahexaenoic acid domains: the ultimate non-raft membrane domain. *Chem. Phys. Lipids* **2008**, *153*, 57–63.

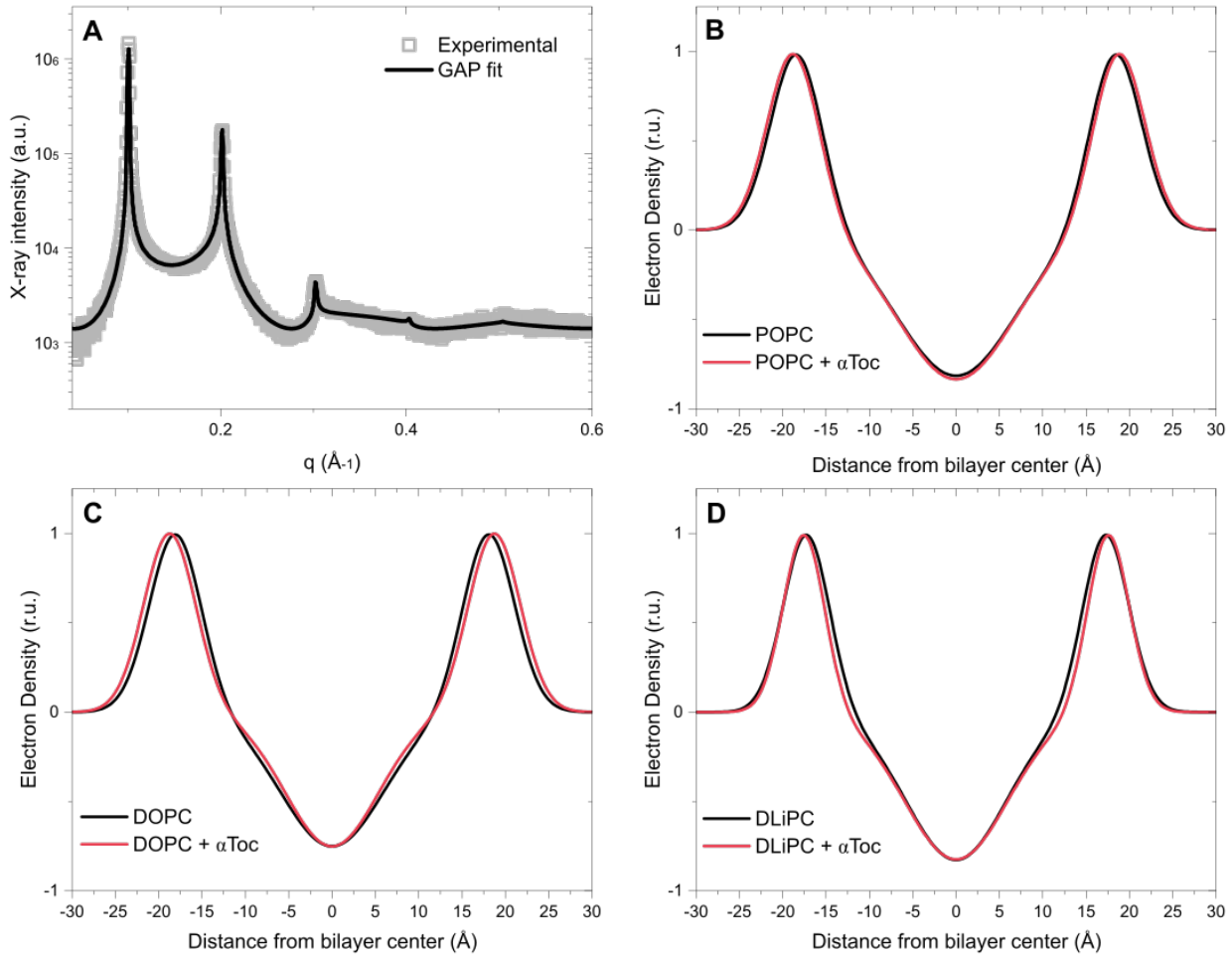

Figure 1: **A** SAXS curve of DOPC MLVs at 20°C. The open squares are the experimental data, and the solid line is the fit from the GAP analysis. Panels **B**, **C** and **D** are the electron density profiles of POPC, DOPC, and DLiPC respectively. The black curves are reconstructions of pure lipid and the red curves are lipid with 10 mol% αToc.

Graphical TOC Entry

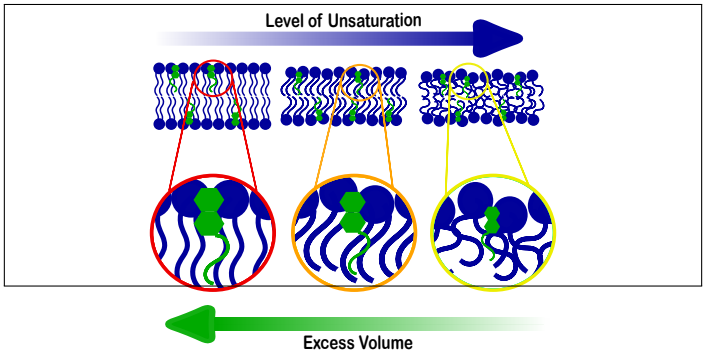

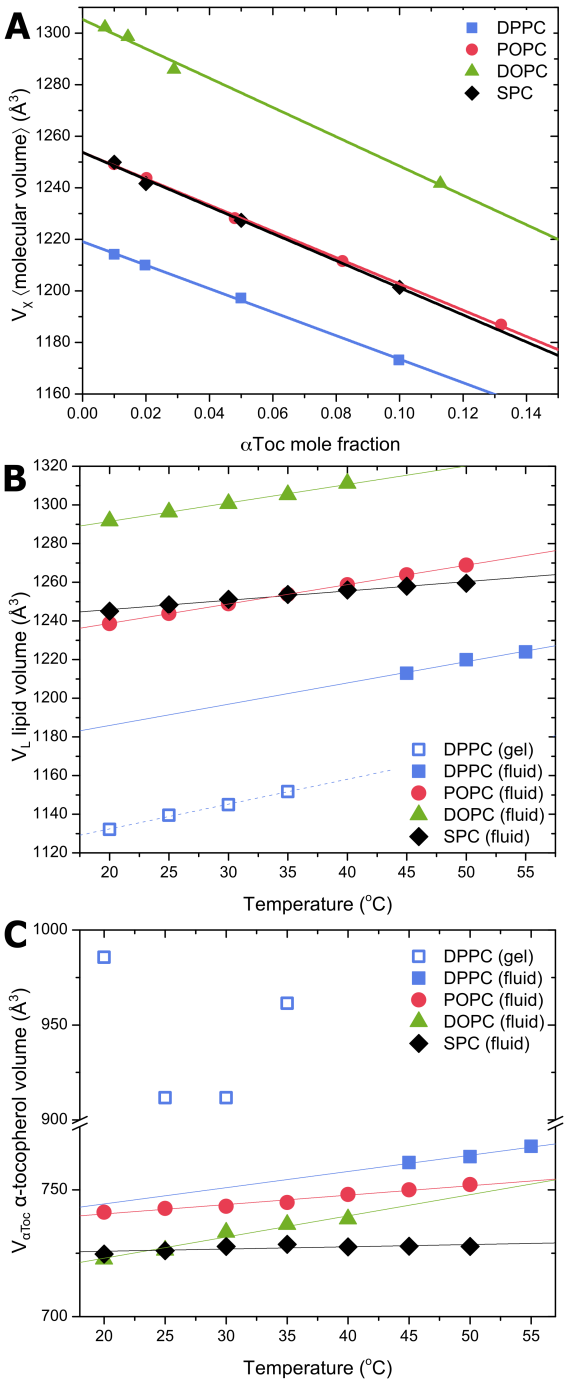

Figure 2: **A**) Average molecular volumes of lipid-αToc mixtures as determined directly from density measurements. The data are for measurements at 35°C for POPC, DOPC, and SPC and 50°C for DPPC. **B**) Volume per lipid of DPPC, POPC, DOPC, and SPC in the presence of αToc at different temperatures. Volumes were determined from the linear fits from panel **A** at $\chi_{\alpha Toc}$=0. Linear fits of the data are added for viewing ease. **C**) Volume per molecule of αToc in DPPC, POPC, DOPC, and SPC at different temperatures. Volumes were determined from the linear extrapolation from panel **A** at $\chi_{\alpha Toc}$=1. Linear fits are provided for viewing ease.

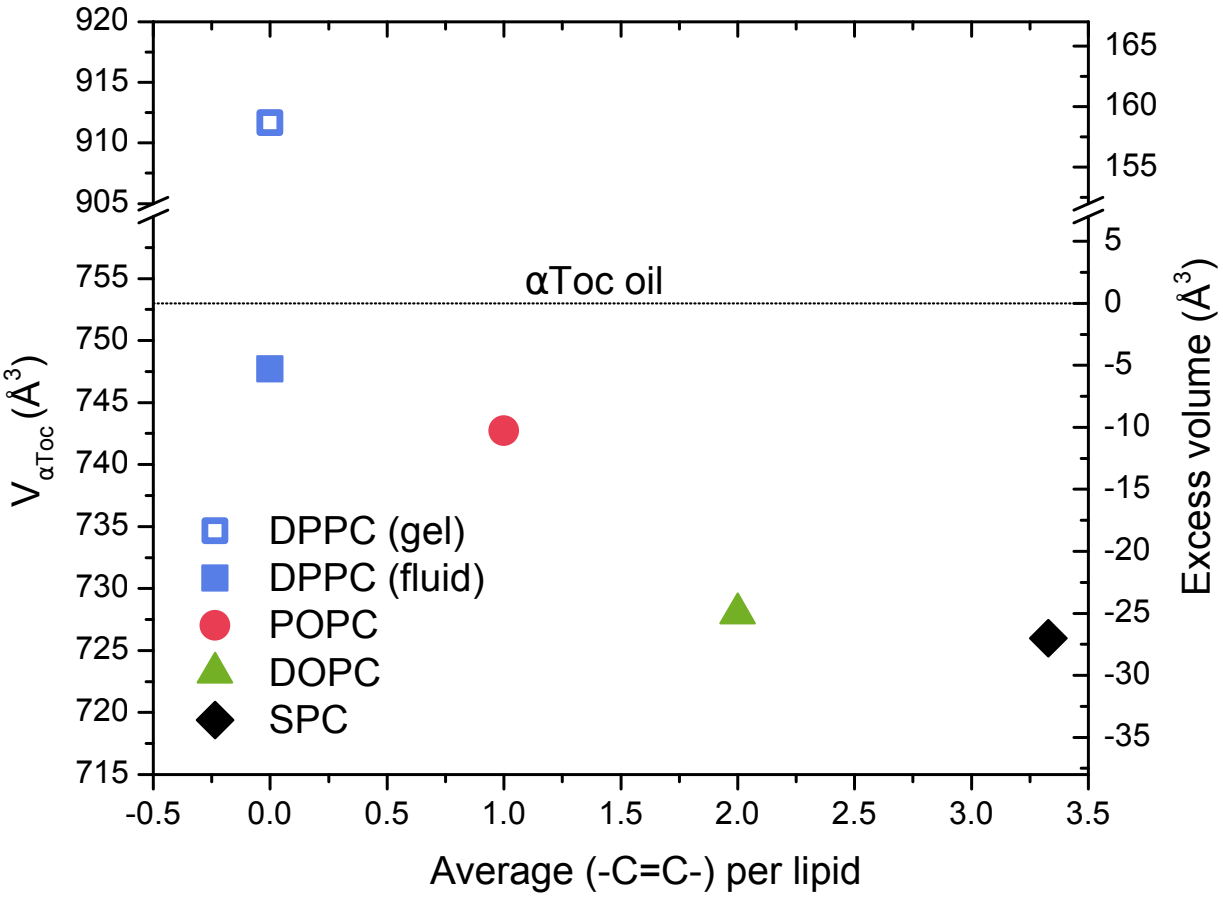

Figure 3: The **left ordinate** represents $V_{\alpha Toc}$ in DPPC, POPC, DOPC, and SPC at 25°C; fluid DPPC values (solid square) were determined from linear extrapolation of experimental fluid phase DPPC data. The horizontal dashed line serves as a reference representing the $V_{\alpha Toc}$ determined from the density of αToc oil at 25°C ($V_{\alpha Toc} = 753$ Å^3). The **right ordinate** is the excess volume of αToc upon mixing in the different lipid species. The abscissa is the average number of carbon–carbon double bonds (-C=C-), or degrees of unsaturation, per lipid. Note the value for SPC was determined based on the fatty acid distribution of the PC extract determined from Orsavova et al..[28]